JOM, Vol. 69, No. 2, 2017
DOI: 10.1007/s11837-016-2199-0

Optical Parameters of Spray-Deposited $CdS_{1-y}Te_y$ Thin Films

SHADIA J. IKHMAYIES[1,2]

1.—Department of Physics, Faculty of Science, Al Isra University, Amman 11622, Jordan. 2.—e-mail: shadia_ikhmayies@yahoo.com

CdS_xTe_{1-x} and $CdS_{1-y}Te_y$ solid solutions are usually formed in the interfacial region in CdS/CdTe solar cells during the deposition of the CdTe layer and/or the processing steps of the device. In this work, indium-doped $CdS_{1-y}Te_y$ thin films were prepared by first producing CdS:In thin films by the spray pyrolysis technique on glass substrates, then annealing the films in nitrogen atmosphere in the presence of elemental tellurium. The films were characterized by scanning electron microscopy, energy dispersive x-ray spectroscopy, and transmittance measurements. The transmittance was used to deduce the reflectance from which the optical parameters were computed. The extinction coefficient, refractive index, the real and imaginary parts of the dielectric constant, optical conductivity, and energy loss were computed, and their dependence on the composition was investigated. In addition, the dispersion of the refractive index was analyzed by the single oscillator model, and dispersion parameters were investigated.

INTRODUCTION

Polycrystalline thin-film CdS/CdTe solar cells are promising candidates for low-cost and high-efficiency photovoltaic applications. The fabrication process of these cells involves the deposition of a *p*-type CdTe absorber layer on top of an *n*-type CdS one which acts as a window. To improve the conductivity of the window layer, it is recommended to dope it with certain dopants such as indium. During the fabrication of the CdTe layer and/or during the post-deposition heat treatment of the device, interdiffusion of CdS and CdTe at the CdS/CdTe junction takes place. The results of this process are the formation of a CdS_xTe_{1-x} layer, which is Te-rich on the CdTe side, and a $CdS_{1-y}Te_y$ layer, which is S-rich on the CdS side. These interdiffusion processes have largely been realized to significantly improve the device performance, where they modify the spectral response of the solar cell. That is, a 10% lattice mismatch exists between CdS and CdTe, which should generate a large density of defects,[1] and produce strain at the CdS/CdTe interface.[2] Intermixing at the CdS/CdTe interface is expected to reduce the effect of lattice mismatch, and, when it relieves strain, reduces the number of interfacial states and the number of recombination centers,[3] thus enhancing the solar cell performance. Hence, a complete understanding of the compositional, structural, electrical, and optical properties of the intermixed layers, CdS_xTe_{1-x} and $CdS_{1-y}Te_y$, which usually constitute the interfacial region in the CdS/CdTe solar cell is essential.

Thin films of CdS_xTe_{1-x} and $CdS_{1-y}Te_y$ have been deposited by different methods, such as thermal evaporation,[4–6] pulsed electrodeposition,[7] brush plating,[8] closed space sublimation,[9] and the spray pyrolysis technique (SP).[3,10] In this work, $CdS_{1-y}Te_y$ thin films were prepared by first producing CdS:In thin films by the spray pyrolysis technique, then annealing them in a nitrogen atmosphere in the presence of tellurium vapor. This method was used because it is easy, cheap, and enables the production of large-area films. The aims of this work are to produce $CdS_{1-y}Te_y$ thin films, deduce the optical parameters, and study the dependence of these parameters on the composition of the films. The extinction coefficient, refractive index, dispersion parameters, the real and imaginary parts of the dielectric constant, optical conductivity, and energy loss were deduced and investigated.

EXPERIMENTAL PROCEDURE

Polycrystalline indium-doped cadmium sulfide (CdS:In) thin films were first deposited onto glass substrates with the spray pyrolysis technique by

(Published online November 28, 2016)

using a precursor solution formed from stoichiometric ratios of thiourea [$(NH_2)_2CS$] and the hydrated cadmium chloride ($CdCl_2{\cdot}H_2O$) dissolved in distilled water with indium chloride ($InCl_3$) as a doping compound. To produce $CdS_{1-y}Te_y$ films, the CdS:In thin films were annealed in a nitrogen atmosphere in the presence of elemental tellurium. Different ratios of tellurium in the films were obtained by changing the period of annealing. A double-beam Shimadzu UV 1601 (PC) spectrophotometer was used to measure the transmittance of the films with respect to a piece of glass similar to the substrates. The microstructure of the films was determined by scanning electron microscopy (SEM), and the composition was determined by energy dispersive x-ray spectroscopy (EDS). SEM observations and EDS analysis were taken by a FEI scanning electron microscope (Inspect F 50) which is supported by energy dispersive x-ray spectroscopy. The thickness of the films was determined before annealing by using transmittance and Lambert's law of absorption in a semiconductor.

RESULTS AND DISCUSSION

A set of $CdS_{1-y}Te_y$ thin films of comparable thickness and different tellurium content were produced. The thickness and composition y of the films have been inserted in Table I, in which y = [Te]/([S] + [Te]), where [Te] and [S] refer to the concentrations of Te and S in the films, respectively, and were obtained from the EDS reports. The films were doped with indium, because the window layer is usually doped with a certain dopant such as indium to increase its conductivity, which means that the solid solution will be doped with the same dopant. The percentage ratios of the concentration of indium to that of cadmium ([In]/[Cd])% in the solution and in the films are also listed in Table I.

Figure 1 displays the SEM micrographs of a CdS:In film and $CdS_{1-y}Te_y$ films of comparable thickness but different composition. The difference between the morphologies of the CdS:In film and the $CdS_{1-y}Te_y$ films is apparent, with the grains of the CdS:In film being large (100–200 nm) and obvious, and the film appears to be compact and uniformly covered with material. On the other hand, the surfaces of the $CdS_{1-y}Te_y$ films appear to consist of smaller grains and aggregates of smaller grains, and they contain some pores.

To explore the optical parameters of the films, the transmittance was recorded at room temperature in the wavelength range 290–1100 nm and is displayed as a function of wavelength λ in Fig. 2. As shown, the highest transmittance is that of the CdS:In film, and it decreases with y. In addition, it is obvious from the figure that the absorption edge shifts towards the side of the longer wavelength, and its sharpness decreases with y. These observations can be interpreted by comparing the band gaps of CdS:In (2.5 eV) and CdTe (1.5 eV). So, the increase of Te content of the films increases the absorption and decreases the transmission. As a result, the absorption edge shifts to the lower energy side, or in other words from the absorption edge of CdS:Into that of CdTe, but the relationship is not linear.[11]

To find the refractive index and the extinction coefficient, the definition of the reflectance of a film for a light wave incident normally from air, with refractive index $n_0 = 1$, on a medium of complex refractive index n^*, is used. Reflectance is given by the following relationship;[5]

$$R = \frac{(n^* - 1)^2}{(n^* + 1)^2} = \frac{(n-1)^2 + k^2}{(n+1)^2 + k^2} \quad (1)$$

The complex refractive index of the film is given by;

$$n^* = n + ik \quad (2)$$

where n is the refractive index and k the extinction coefficient of the film.

Reflectance was deduced from transmittance spectra using the relationship $T + R = 1$. Figure 3 depicts the relationship between R and photon's energy, hν. As shown, there is a shift of the absorption edge towards smaller energy with the increase of y. The reflectance before the absorption edge of each film is smaller than that after it, and R increases with hν. Also, in this region, R increases with Te content in the films (y). At the absorption edge of each film, there is a sharp increase in R, where the sharpness of the absorption edge decreases with y due to the mixed phase (cubic and hexagonal) of the $CdS_{1-y}Te_y$ solid solution.[3,10] The reflectance becomes constant equal or close to 1 after the absorption edge of each film.

Knowing the value of the absorption coefficient α, which can be deduced from the transmittance, the extinction coefficient can be calculated using the relationship

Table I. The thickness t, composition y, and ratios of indium to cadmium concentrations in the precursor solution and in the films, respectively

t (nm)	$y \times 10^{-2}$	([In]/[Cd])% in the solution	([In]/[Cd])% in the film
500	0	1.5	3.31 ± 0.34
490	3.49 ± 1.68	1.5	2.98 ± 0.20
465	8.52 ± 6.41	1.5	3.84 ± 0.63
420	9.97 ± 9.21	0.1	2.75 ± 1.88
460	10.02 ± 8.27	0.0055	3.08 ± 1.24

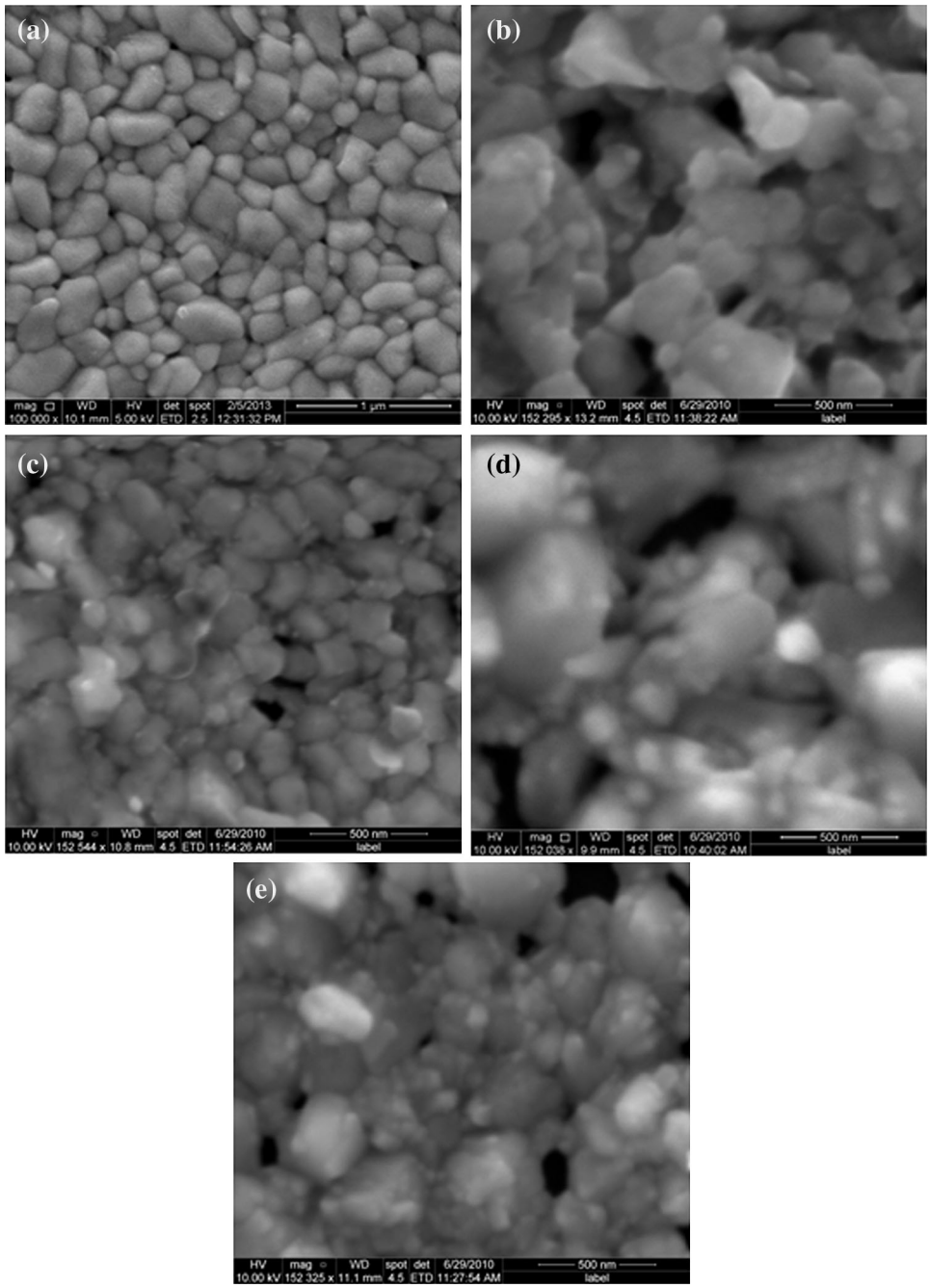

Fig. 1. The SEM micrographs of $CdS_{1-y}Te_y$ thin films for $y = 0.0$ (CdS:In) (a), $y = 3.49 \times 10^{-2}$ (b), $y = 8.52 \times 10^{-2}$ (c). $y = 9.97 \times 10^{-2}$ (d), and $y = 10.02 \times 10^{-2}$ (e). In (a), the scale is 1 μm, but in (b)–(e) it is 500 nm.

$$k = \frac{\lambda\alpha}{4\pi} \tag{3}$$

where λ is the wavelength in free space. Solving Eq. 1 for the refractive index n gives;

$$n = \frac{(1+R) + \left[(1+R)^2 - (1-R)^2\left(1+k^2\right)\right]^{1/2}}{1-R} \tag{4}$$

The extinction coefficient k is calculated from Eq. 3 and plotted against the photon's energy hν and displayed in Fig. 4. The extinction coefficient shows a non-zero value in the region below 2.5 eV. It is well known in the case of polycrystalline films that extra absorption of light occurs at the grain boundaries, which leads to non-zero values of k for photon energies smaller than the fundamental absorption edge.[12] In this region, k is restricted in the range 0.042–0.174, where it increases with y. A sharp increase in k occurs at the absorption edges which vary according to y. As seen in Fig. 2, the absorption edge shifts to the lower energy side with y, and the films with $y = 9.97 \times 10^{-2}$ and $y = 10.02 \times 10^{-2}$ show two absorption edges, which are not obvious in

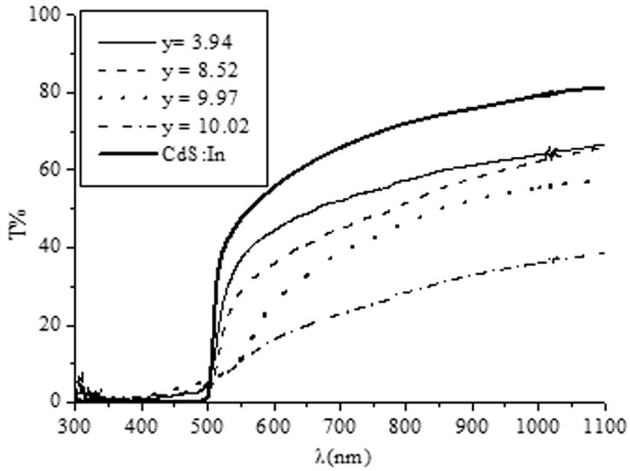

Fig. 2. Transmittance of $CdS_{1-y}Te_y$ thin films of different composition y and comparable thickness besides that of a CdS:In film.

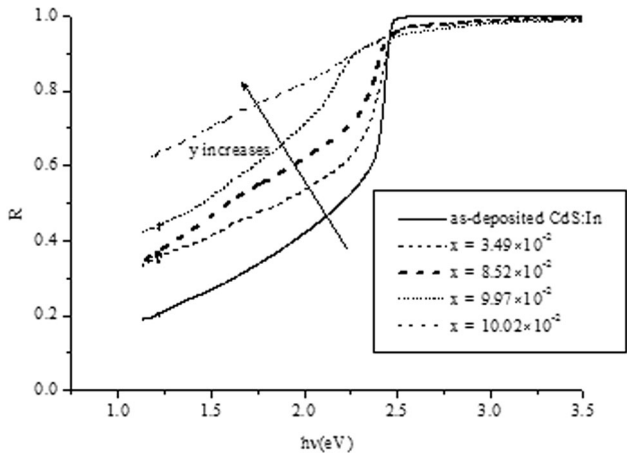

Fig. 3. Reflectance of $CdS_{1-y}Te_y$ thin films of different composition y and comparable thickness besides that of a CdS:In film.

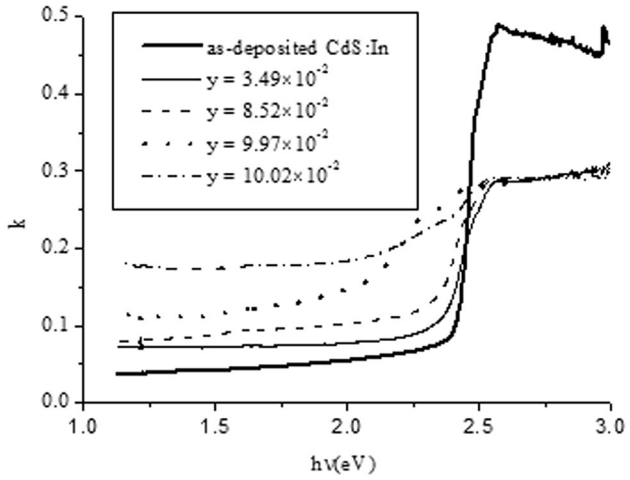

Fig. 4. The extinction coefficient k of a CdS:In film and the $CdS_{1-y}Te_y$ thin films with comparable thickness and different composition y.

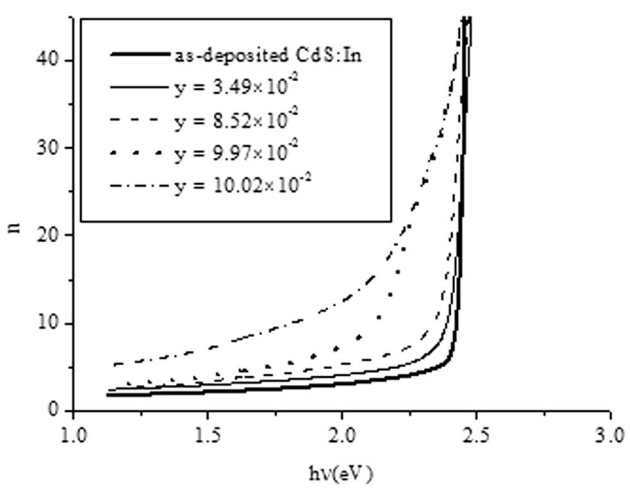

Fig. 5. The refractive index of $CdS_{1-y}Te_y$ thin films of comparable thickness with different composition y.

Figs. 2 and 3. These are due to the presence of a mixed phase in the films (cubic and hexagonal), where the cubic phase has a slightly smaller optical bandgap.[3,10] After the sharp increase, k becomes constant and equal to 0.291 for all $CdS_{1-y}Te_y$ films. For the CdS:In film, k slowly decreases with hν from 0.487 to 0.453 for the energy change from 2.5 to 3.0 eV.

The refractive index n is calculated from Eq. 4 and is plotted against the photon's energy hν as displayed in Fig. 5. It can be observed that n increases slowly with hν until the absorption edge, which depends on y, after which it strongly increases with hν, and then reaches an approximately constant value, not shown in the figure. It is obvious that the sharpest absorption edge is that of the CdS:In thin film, then the sharpness decreases with y. The shift of the absorption edge towards lower energy is also observed. As the Figure shows, for energies less than ≈2.25 eV, the refractive index

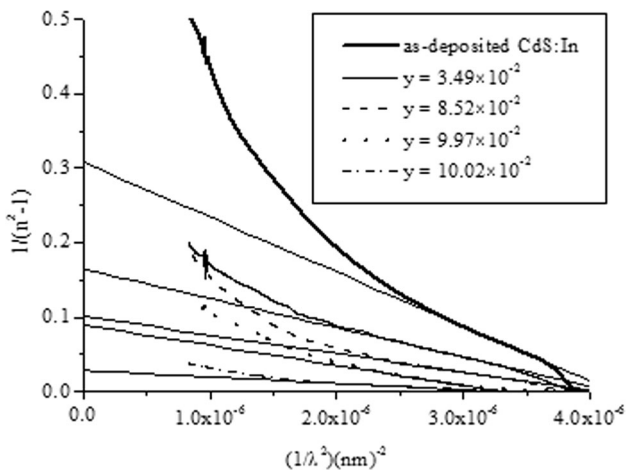

Fig. 6. The plot of $(n^2 - 1)^{-1}$ against λ^{-2} for a CdS:In film and the $CdS_{1-y}Te_y$ thin films of different composition y.

Table II. The optical parameters of $CdS_{1-y}Te_y$ thin films with the thickness and composition of each film

t (nm)	Composition y	n_∞	ε_∞	λ_0 (nm)	E_0 (eV)	E_d (eV)	M_{-1} $(eV)^{-2}$	M_{-3} $(eV)^{-2}$
500	0	1.628	2.649	591.7	2.096	3.457	1.649	0.376
490	3.49 ± 1.68	2.208	4.873	591.9	2.095	8.115	3.873	0.882
465	8.52 ± 6.41	2.177	4.740	666.3	1.861	6.960	3.740	1.080
420	9.97 ± 9.21	2.548	6.495	648.9	1.911	10.500	5.495	1.505
460	10.02 ± 8.27	4.321	18.671	667.3	1.858	32.838	17.671	5.117

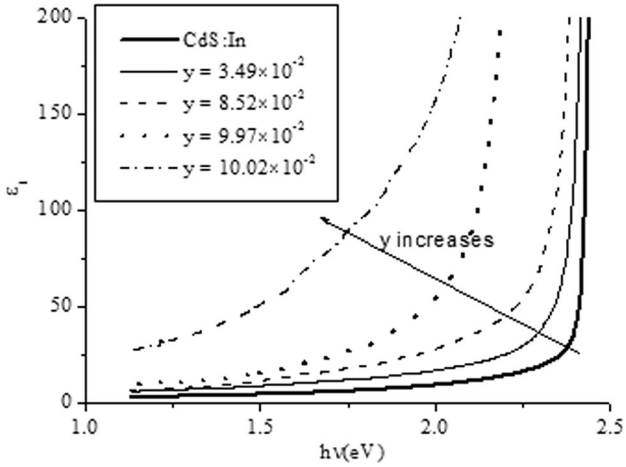

Fig. 7. The real part of the dielectric constant of $CdS_{1-y}Te_y$ thin films of comparable thickness but different composition.

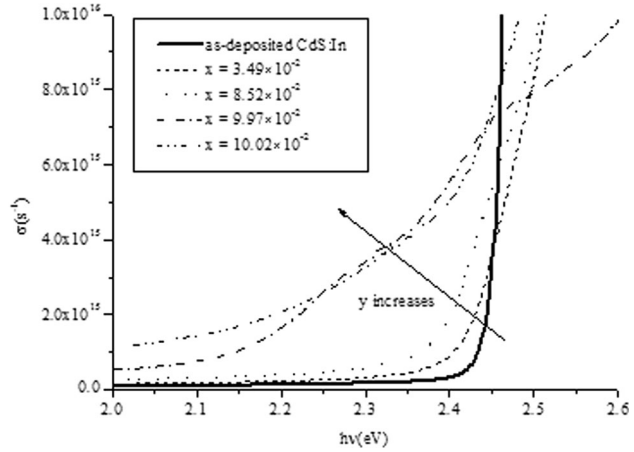

Fig. 9. The optical conductivity σ of $CdS_{1-y}Te_y$ thin films of different composition but comparable thickness.

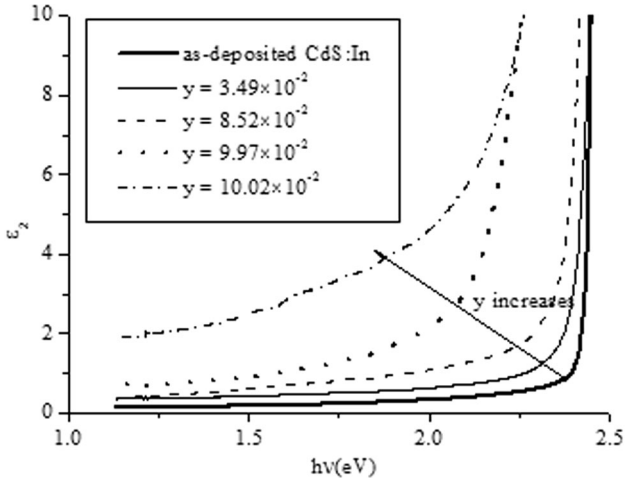

Fig. 8. The imaginary part of the dielectric constant of $CdS_{1-y}Te_y$ thin films of different composition but comparable thickness.

increases slowly with y, and its value in this region at $h\nu = 1.5$ eV, which corresponds to the bandgap energy of CdTe lies in the range 2.10 for as-deposited CdS:Into 7.17 for $y = 10.02 \times 10^{-2}$.

Below the absorption edge, refractive index dispersion can be analyzed by the single oscillator model. So, the obtained data of refractive index n has also been analyzed to yield the long wavelength refractive index (n_∞) together with the average oscillator wavelength (λ_0) for $CdS_{1-y}Te_y$ thin film using the following relationship;[13]

$$\frac{n_\infty^2 - 1}{n^2 - 1} = 1 - \left(\frac{\lambda_0}{\lambda}\right)^2 \tag{5}$$

The relationship between $(n^2 - 1)^{-1}$ and λ^{-2} is shown in Fig. 6, beside the linear fits in the linear parts of the curves, where λ_0, n_∞ and $\varepsilon_\infty = n_\infty^2$ are evaluated from the fit parameters and listed in Table II. From these values, the average excitation energy for electronic transitions $E_0 = hc/\lambda_0$, and the dispersion energy which is a measure of the strength of interband optical transitions $E_d = E_0(n_\infty^2 - 1)$, are also calculated and listed in Table II. In addition, the M_{-1} and M_{-3} moments of the optical spectrum which measure the interband transitions can be obtained from the two equations;[13]

$$E_0^2 = \frac{M_{-1}}{M_{-3}} \tag{6}$$

$$E_d^2 = \frac{M_{-1}^3}{M_{-3}} \tag{7}$$

From Table II, it can be observed that n_∞, ε_∞, E_d, M_{-1} and M_{-3} increase with the Te content of the films (y).

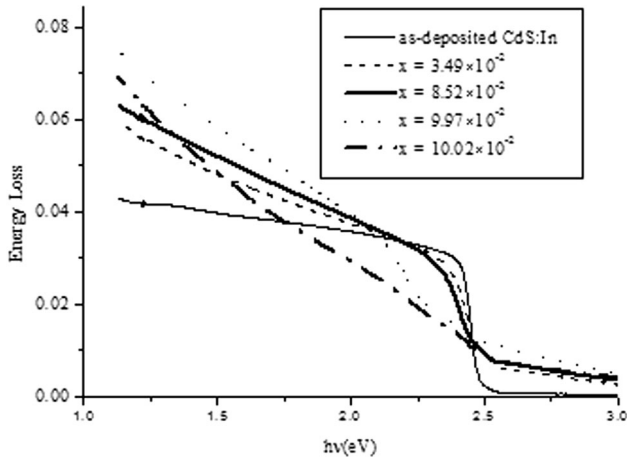

Fig. 10. The energy loss against photon's energy hν of CdS_yTe_{1-y} thin films of different composition but comparable thickness.

The complex dielectric constant $\varepsilon^* = \varepsilon_1 + i\varepsilon_2$, where i is the square root of -1 is a fundamental intrinsic material property. The real part ε_1 is associated with the refractive index and hence the speed of light in the material. The imaginary part of the dielectric constant ε_2 is related to the absorption of light in the material. The real and imaginary parts of the dielectric constant are determined by using the following equations;[14]

$$\varepsilon_1 = n^2 - k^2 \tag{8}$$

$$\varepsilon_2 = 2nk. \tag{9}$$

Figure 7 displays the real part of the dielectric constant ε_1 against the photon's energy hν for $CdS_{1-y}Te_y$ films with comparable thickness but different composition y. In the region below 1.5 eV, ε_1 increases with y, where it varies at hν = 1.15 eV from 2.99 to 28.21. It increases gradually with hν, and then sharply increases around the region of the absorption edge of each film. The absorption edge moves towards lower energy with the increase in y. These observations are consistent with the behavior of the refractive index n and have the same explanations.

Figure 8 displays the imaginary part of the dielectric constant ε_2 against the photon's energy hν for the same set of films. In the low energy side at hν = 1.25 eV, it increases with y and varies in the range 0.127–1.913, and it increases slowly with hν. In the region of the absorption edge, ε_2 increases sharply with hν, where the rate of increase decreases with y. The presence of the two phases of the $CdS_{1-y}Te_y$ solid solution causes the decrease in the increasing rate of ε_2. In the high-energy side after 2.5 eV, ε_2 becomes constant and consistent with the behavior of the extinction coefficient k. Both the real and imaginary parts of the dielectric constant show similar behaviors, but the imaginary part displays smaller values.

The optical conductivity σ of the $CdS_{1-y}Te_y$ thin films can be determined using the formula;[15]

$$\sigma = \frac{\alpha nc}{4\pi} \tag{10}$$

where $c$is the speed of light. Figure 9 displays the optical conductivity σ of the whole set of films under study as a function of the photon's energy hν. From the Figure, it is obvious that, before the absorption edge, σ is constant close to zero for CdS:In film, but non-zero for $CdS_{1-y}Te_y$ thin films, and it increases with y. The optical conductivity σ slowly increases with hν, and this increase becomes faster as y increases. It strongly increases at the absorption edge, and the sharpness of this increase decreases with Te content of the films (y). As seen before, the absorption edge shifts towards lower energy with y, and the presence of the two phases in the $CdS_{1-y}Te_y$ films is apparent for the upper two curves which have the largest values of y, where two non-sharp absorption edges can be seen, which are related to the mixed phase of the films. After the absorption edge in the high-energy side σ of $CdS_{1-y}Te_y$ films takes large values that increase with y (1×10^{16} – 1.8×10^{16}), while that of the CdS:In thin film takes a higher value of 4.1×10^{17}, where these values are not shown in Fig. 9. The enhanced optical conductivity at the lower wavelengths is due to the high absorbance of the films in that region.[12]

Dielectric loss is a loss of energy that goes into heating a dielectric material in a varying electric field. The dielectric loss is given by the relationship;[13]

$$\tan\delta = \frac{\varepsilon_2}{\varepsilon_1}, \text{ and the loss angle is } \delta = \tan^{-1}\left(\frac{\varepsilon_2}{\varepsilon_1}\right). \tag{11}$$

Figure 10 depicts the energy loss against the photon's energy hν of CdS_yTe_{1-y} thin films of different composition y, but comparable thickness. It is apparent that the energy loss decreases with hν before, around, and after the absorption edges of each film. In general, the energy loss increases with y, where it has largest values at $y = 9.97 \times 10^{-2}$, but smallest values for $y = 0$ (the as-deposited CdS:In film). The influence of the Te content of the films on the absorption edges is also obvious, where the sharpness decreases with y due to the presence of the mixed phase. After the absorption edge, the energy loss is constant and equal to zero for the CdS:In thin film, but it is non-zero, and decreasing with hν for the $CdS_{1-y}Te_y$ thin films.

CONCLUSION

$CdS_{1-y}Te_y$ thin films were produced by first preparing CdS:In thin films by the spray pyrolysis technique on glass substrates, then annealing these films in the presence of elemental Te in nitrogen atmosphere at 400°C. The composition of the films

was revealed by EDS. SEM micrographs showed that the films are polycrystalline. The transmittance of the films was used to get their optical parameters such as the absorption coefficient, extinction coefficient, refractive index, real and imaginary parts of the dielectric constant, dispersion parameters, energy loss, and optical conductivity. All these parameters have been found to increase with the composition y, except the energy loss which decreases with y. These results are important for the development of CdS/CdTe solar cells.

REFERENCES

1. R. Dhere, X. Wu, D. Albin, C. Perkins, H. Moutinho, and T. Gessert, *Formation and characterization of CdS_xTe_{1-x} alloys prepared from thin film couples of CdS and CdTe*. Paper presented at the 29th IEEE PV specialists conference, New Orleans, Louisiana, 20–24 May 2002.
2. J.N. Duenow, R.G. Dhere, H.R. Moutinho, B. To, J.W. Pankow, D. Kuciauskas, and T.A. Gessert, *Proceedings of the 2011 Materials Research Society Spring Meeting*, San Francisco, CA, 25–29 April 2011.
3. S.J. Ikhmayies and R.N. Ahmad-Bitar, *Sol. Energy* 86, 2613 (2012).
4. G. Gordillo, F. Rojas, and C. Calderón, *Superf. Vasio* 16, 30 (2003).
5. S.S. Babkair, N.M. Al-Twarqi, and A.A. Ansari, *Karachi Univ. J. Sci.* 39, 1 (2011).
6. D.A. Wood, K.D. Rogers, D.W. Lane, and J.A. Coath, *J. Phys. Condens. Mater.* 12, 4433 (2000).
7. K.R. Murali, P. Thirumoorthy, C. Kannan, and V. Sengodan, *Sol. Energy* 83, 14 (2009).
8. R. Marymathelane, Ritajohn, and K.R. Murali, *Int. J. Eng. Sci. (Ijes)* 2, 14 (2013).
9. M.S. Kale, Y.R. Toda, and D.S. Bhavsar, *IOSR J. Appl. Phys. (IOSR-JAP)* 6, 22 (2014).
10. S.J. Ikhmayies and R.N. Ahmad-Bitar, *J. Lumin.* 132, 2826 (2012).
11. R. Pal, J. Dutta, S. Chaudhri, and A.K. Pal, *J. Phys. D Appl. Phys.* 26, 704 (1993).
12. P.P. Sahay, R.K. Nath, and S. Tewari, *Cryst. Res. Technol.* 42, 275 (2007).
13. E.Ş. Tüzemen, S. Eker, H. Kavak, and R. Esen, *Appl. Surf. Sci.* 255, 6195 (2009).
14. A.A. Alnajjar, F.Y. Al-Shaikley, and M.F.A. Alias, *J. Electron Device* 16, 1306 (2012).
15. R.L. Mishra, S.K. Mishra, and S.G. Prakash, *J. Ovonic Res.* 5, 77 (2009).